Philosophical Magazine
Vol. 89, Nos. 28–30, 1–21 October 2009, 2599–2621

Taylor & Francis
Taylor & Francis Group

Limiting factors in the fabrication of microcrystalline silicon solar cells and microcrystalline/amorphous ('micromorph') tandems

F. Meillaud[a]*, A. Feltrin[a], D. Dominé[a], P. Buehlmann[a], M. Python[a], G. Bugnon[a], A. Billet[a], G. Parascandolo[a], J. Bailat[b], S. Fay[a], N. Wyrsch[a], C. Ballif[a] and A. Shah[a]

[a]*Institute of Microtechnology (IMT), Breguet 2, 2000 Neuchâtel, Switzerland;* [b]*Oerlikon Solar-Lab S.A., Puits-Godets 6a, 2000 Neuchâtel, Switzerland*

(*Received 4 October 2008; final version received 8 January 2009*)

This contribution presents the status of amorphous and microcrystalline silicon solar cells on glass, and discusses some material/fabrication factors that presently limit their conversion efficiency. Particular attention is focused on recent results and developments at the Institute of Microtechnology (IMT) in Neuchâtel. The performances and stability of microcrystalline silicon single-junction and amorphous/microcrystalline ('micromorph') tandem solar cells are discussed, as a function of material properties. Recent results on the electrical effect of cracks in microcrystalline silicon material are presented. Degradation under the effect of illumination is a well-known limiting factor for amorphous silicon solar cells. As a comparison, studies on the stability of microcrystalline silicon with respect to light-induced degradation are commented upon. The importance of transparent contacts and anti-reflection layers for achieving low electrical and optical losses is discussed. Finally, efforts towards industrialization of micromorph tandem solar cells are highlighted, specifically (i) the development and implementation of an *in situ* intermediate reflector in a large-area industrial deposition system, and (ii) recent achievements in increasing the growth rate of microcrystalline silicon.

Keywords: microcrystalline silicone; solar cells; materials preparation; materials characerization; electrical properties; defects in solids

1. Introduction

From a number of aspects, thin film silicon constitutes a promising option for a further cost reduction in photovoltaic (PV) modules. Material requirements are reasonable: no rare or toxic raw materials are used in large quantities, and a lower energy payback time can be attained compared to typical wafer-based PV technology [1]. The development of thin film silicon layers began in the 1960s [2], leading to solar cells in the 1970s [3], but was initially limited to hydrogenated amorphous silicon solar cells (a-Si:H) and its alloys with carbon (a-SiC:H) and germanium (a-SiGe:H). Thin film silicon technology has matured to an industrially viable technology over the past 20 years, although its share of the PV market has, to date, remained

*Corresponding author. Email: fanny.meillaud@unine.ch

ISSN 1478–6435 print/ISSN 1478–6443 online

DOI: 10.1080/14786430902738772
http://www.informaworld.com

below 10%. This should increase in the future, with a more than 20% share expected in 2012, thanks to a dramatic increase in the number of thin film silicon module manufacturers. Hydrogenated microcrystalline silicon (μc-Si:H) was first reported in 1968 [4]. It can be produced using the same equipment as a-Si:H; however, it has quite different material properties [5]. For example, it possesses a lower, indirect bandgap of ~1.1 eV, which leads to lower open-circuit voltage values and to enhanced absorption in the near infrared part of the solar spectrum. However, due to the indirect bandgap, thicker intrinsic μc-Si:H layers are necessary to obtain sufficient absorption and photogeneration. Also, there are differences in (coplanar) electronic transport, which are limited in μc-Si:H layers by defects present at the boundaries of the crystalline phase, i.e. at the boundaries of crystalline grain conglomerates [6]. For these reasons, it took several years before hydrogenated microcrystalline silicon was employed as an intrinsic photo-generation layer in solar cells [7,8]. Indeed, μc-Si:H was initially only used for doped layers in single-junction a-Si:H solar cells. In the 1990s, promising, entirely microcrystalline p-i-n (superstrate) and n-i-p (substrate)-type silicon solar cells were fabricated, rapidly reaching initial conversion efficiencies higher than 7% [9,10]. Alloys of microcrystalline silicon with carbon were also developed at this time [11,12]. In laboratory tests, the best μc-Si:H single-junction solar cells currently attain conversion efficiencies in the order of 10% [13,14], with a record, confirmed initial efficiency of 10.1% for 2 μm on glass and a cell area of 1.2 cm^2 [15]. On the other hand, the best, confirmed stabilized efficiency for single-junction a-Si:H solar cells is equal to 9.5% for a 1-cm^2 test cell [16], whereas an initial value of 128.8 W and an expected stabilized output power of ~100 W have been presented for 1.4-m^2 a-Si:H modules [17]. The a-Si:H/μc-Si:H tandem solar cell, usually known as a 'micromorph' or 'hybrid', was first introduced at IMT Neuchâtel. Initial results were reported in 1994 [18], and stabilized efficiencies larger than 10% had already been confirmed and reported in 1997 [19]. Currently, stable efficiencies reach values of between 10 and 12% [20–22], whereas Kaneka Corp. have announced an initial efficiency up to 14.7% [23] and a best confirmed stable value of 11.7% [24].

This contribution will examine the fabrication and basic properties of thin microcrystalline silicon layers and solar cells. Due to the complexity of the material, many aspects of μc-Si:H are still under investigation, some of which will be presented here. Recent developments in large area industrial R&D systems will be considered. The results of larger deposition rates for μc-Si:H, together with the development of an *in situ* intermediate reflector for the micromorph tandem, will also be discussed.

2. Deposition techniques for amorphous and microcrystalline silicon

As opposed to thin film polycrystalline material, amorphous and microcrystalline silicon are deposited at low temperatures (~200°C) from gaseous precursors, typically from silane (SiH_4) and hydrogen (H_2). A usual deposition technique is plasma-enhanced chemical vapor deposition (PECVD), which commonly takes place in a capacitively-coupled reactor. In such reactors, the plasma is generally excited via an AC signal at a frequency equal to the standard radio frequency (RF) value of 13.56 MHz. By increasing the plasma excitation frequency from 13.56 to ~70 MHz

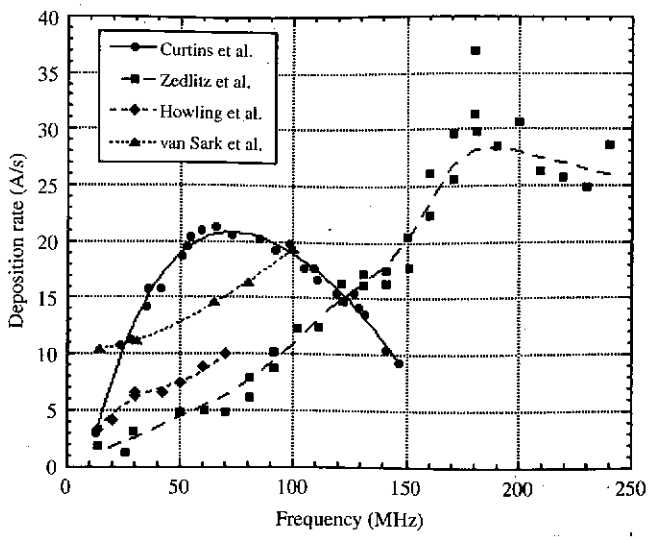

Figure 1. Deposition rate of amorphous silicon layers versus plasma excitation frequency, as obtained in different reactors and by independent research groups [25–28].

(very high frequency, VHF), the deposition rate of amorphous silicon layers can be dramatically increased, as can be seen in Figure 1, where results of different groups are presented [25–28]. For microcrystalline silicon, a recent survey by Smets et al. [29] showed that larger deposition rates are also reported for the VHF, compared to the RF regime, particularly when high deposition pressures are used. In addition, by increasing the frequency, one raises the 'powder limit', i.e. the maximum power level or maximum deposition rate above which a significant amount of powder is formed in the plasma [27]. With increased plasma excitation frequency, a reduction in sheath thickness and a change in ion bombardment are observed, with a reduction of the maximum energy of ions reaching the growing surface [30]. Furthermore, for constant effective plasma power, an increase in the optical emission line of SiH* radicals is clearly observed with increased frequency values. A direct correlation between SiH* intensity and deposition rate have been reported by Howling et al. [28], which is attributed to a more effective silane dissociation within the plasma. Thus, SiH* can be used as an indicator of local spatial variation in deposition rates, with a better film uniformity achieved at higher frequencies. Note that at fixed input (not effective) power, a decrease in deposition rate is observed for larger frequencies, which is attributed to a less efficient power coupling within the reactor, a decrease in electron density or depletion of SiH_4 in the feed gas [25,26]. van Sark et al. [28] showed that the monotonous increase of deposition rate with frequency was justified by surface reactions induced by ion impacts. Indeed, the flux of ions of lower energy increases with increasing excitation frequency, a phenomenon that leads, according to the authors [28], to a higher density of vacant sites and, hence, a larger deposition rate. Ion bombardment, and its possible detrimental effect on material quality, will also be discussed as a function of deposition pressure for μc-Si:H material fabrication. Indeed, various plasma regimes can be used for μc-Si:H material, one being the high pressure depletion (HPD) regime. In this regime, pressures up to

10 Torr are used with high silane depletion conditions, combined with RF [31,32] or VHF excitation frequencies [33,34]. Under such conditions, the deposition rate can be significantly increased to over 10 Å/s, while producing high-quality μc-Si:H cells with efficiencies up to 9.8% [13]. Moreover, single-junction solar cells with efficiencies in the order of 9% have been obtained at rates ranging between 20 and 40 Å/s [34,35].

Over the years, a large number of deposition techniques other than PECVD have been developed, including (i) the hot wire (HW) deposition technique and (ii) the microwave plasma regime. In the case of HW, the silane gas is thermally dissociated using a metal filament (commonly tungsten or tantalum) heated to temperatures above 1500°C. Since there is no plasma, ion bombardment is completely avoided. This may be a drawback, however, since a certain amount of low-energy ion bombardment is beneficial for microcrystalline silicon growth. Furthermore, deposition temperature control is difficult since the substrate and growing layer are exposed to thermal radiation from the filament. This is especially critical if the substrate is placed near the filament, as is the case when increased deposition rates are desired. In the HW regime, high deposition rates have been obtained for individual layers [36] but higher solar cell efficiencies, up to 9.4%, have been produced only at low rates [37]. The most promising results have, to date, been obtained when combining hot wire with VHF PECVD, with conversion efficiencies up to 8.1% at 12 Å/s [38]. Hot wire can additionally be used as a deposition technique for the buffer layer at the p/i interface in μc-Si:H PECVD solar cells, leading to initial efficiencies up to 10.3% [39].

In microwave plasma, ion bombardment is reduced compared to standard RF plasma deposition and high deposition rates can also be achieved. Nevertheless, no significant results on exclusively μc-Si:H solar cells have been reported as yet [40,41].

3. Thin film silicon material properties

3.1. *Structure and defects*

As previously mentioned, microcrystalline silicon material is typically deposited from a mixture of silane and hydrogen. The silane concentration (SC), defined as the ratio of silane gas flow over silane + hydrogen flows, i.e. $SC = SiH_4/(SiH_4 + H_2)$, is a major deposition parameter, directly linked to crystallinity of the layer. Low silane concentrations (typically SC ~5–10%) lead to μc-Si:H material, whereas high SC values lead to completely amorphous silicon; the threshold value being unique for each system and each deposition regime. It is possible to deposit μc-Si:H from a pure silane plasma but an amorphous incubation layer is usually formed, lowering the solar cell performances [42]. A more recent study [43] has shown, however, that the amorphous incubation layer can be suppressed by, for example, applying a H_2 flow prior to plasma ignition to suppress SiH_4 back diffusion from the background chamber volume. Efficiencies up to 9.5% could then be reached for single-junction μc-Si:H solar cells.

The evolution of layer crystallinity with increasing hydrogen dilution can be observed microscopically by transmission electron microscopy (TEM) [44], X-ray diffraction [45] and Raman spectroscopy [46]. Microcrystalline silicon is a very

complex material, composed of silicon nanocrystals embedded in an amorphous phase. The nanocrystals, 10–20 nm in diameter, are generally packed into conglomerates with a diameter of $>0.5\,\mu m$ [6]. Due to nucleation properties, μc-Si:H layer growth depends sensitively on the substrate material and underlying layers on which they are deposited. Indeed, the whole growth process depends on crystallinity but also on the chemical nature and even crystalline orientation of the underlying layers [47–49].

Once the basic process parameters have been adjusted (power, gas flow, etc., leading to a deposition rate yielding high quality material), an optimum in μc-Si:H intrinsic layer quality is typically observed for medium crystalline volume fractions ϕ_c (~40–60%, as determined by Raman spectroscopy with a HeNe laser), as can be seen in Figure 2 both in the initial state and after 1000 h of light-soaking. Here, the reader is referred to a later discussion in this paper about the stability of μc-Si:H. In this case, a series of n-i-p single-junction μc-Si:H solar cells were deposited, for which only the silane concentration of the intrinsic layer was modified. The μc-Si:H material quality was established by Fourier transform photocurrent spectroscopy (FTPS) [50,51]. Using this technique, one can measure the absorption coefficient α of the intrinsic layer for energies ranging 0.6–1.6 eV. The value of α measured at 0.8 eV, which is considered to be the defect-related absorption, is taken as an estimate of the density of recombination centers within the bandgap [52]. Note that similar techniques for sub-bandgap absorption measurements, such as the constant photocurrent method (CPM) or photothermal deflection spectroscopy (PDS), are regularly used to characterize amorphous silicon. In this case, defect-related absorption is measured at 1.2 eV [53] instead of 0.8 eV as in μc-Si:H. Electron spin resonance (ESR) may also be used to characterize defects in thin film silicon layers: Baia Neto et al. [54] observed

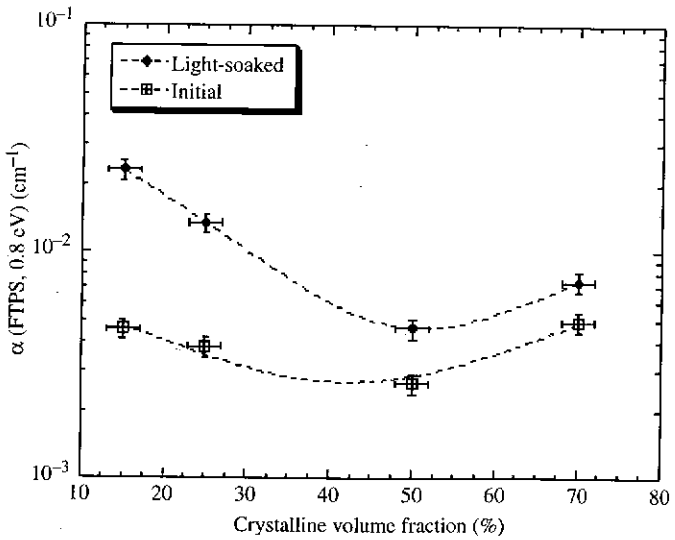

Figure 2. Defect-related absorption in initial and light-soaked state (1000 h under standard conditions) as a function of the intrinsic layer crystalline volume fraction for a dilution series of n-i-p μc-Si:H single-junction solar cells. The dotted lines are guides for the eye.

that several types of defects are present in μc-Si:H, some of which could correspond to surface dangling bonds.

We hence contend that the optimum observed in Figure 2 for a medium value of ϕ_c is related to the passivation of defects, present at the surface of the nanocrystals, by the amorphous silicon phase [55]. Such a passivation mechanism of surface defects by amorphous silicon is well known for amorphous/crystalline interfaces [56] and applied in the Heterojunction with Intrinsic Thin Layer (so-called "HIT") solar cells, commercialized by Sanyo Electric Co.

3.2. *Growth and cell properties*

A μc-Si:H with high material quality (i.e. with low $\alpha = 0.8$ eV and proper crystalline fraction) is, however, not sufficient to ensure good solar cell performance. Indeed, recent studies have demonstrated that additional microstructural defects, growing as cracks, may emerge when challenging substrates are used, such as a highly rough, V-shaped, TCO (transparent conductive oxide) surface [57]. These cracks correspond to zones of porous material. As-grown LPCVD–ZnO is typically a V-shaped material with large, steep pyramids [58]. With this type of substrate, cracks typically appear in the μc-Si:H solar cell at the bottom of the valleys, where pinches are present, as shown in the transmission electron micrograph for a p-i-n single-junction μc-Si:H solar cell deposited on as-grown LPCVD-ZnO (Figure 3a). Here, the crack, designated by an arrow and appearing as a white line, propagates through the entire active part of the device; sometimes it will propagate through part of the i-layer only. However, thanks to an appropriate surface treatment [14], the V-shaped features on the LPCVD–ZnO surface can be turned into U-shape features, with suppression of smaller pyramids or asperities and a smoother morphology (the σ_{RMS} value is thereby decreased from 10 to 25% relatively) (Figure 3b). With this treatment, a dramatic decrease in crack density is observed. Note that cracks have also been observed by other groups in μc-Si:H [59] and a-Si:H [60] solar cells.

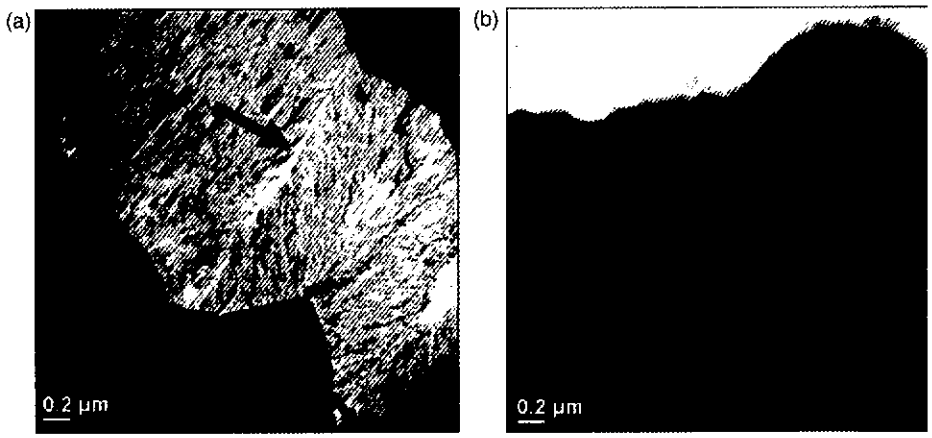

Figure 3. Bright-field TEM cross-section micrographs of μc-Si:H p-i-n on (a) V-shaped and (b) U-shaped substrates, corresponding to the same TCO without (a) and with (b) surface treatment, as presented in [14]. A crack is indicated by the arrow in (a).

We have demonstrated in a recent study [61] that the cracks observed in μc-Si:H solar cells could be considered as an additional source of dark current within the solar cell and, thus, as a second diode, added to the electrical equivalent circuit for a-Si:H solar cells introduced by Merten et al. [62] (Figure 4). The $I(V)$ curve for the μc-Si:H solar cell may then be expressed as the sum of all components (superposition principle):

$$I(V) = I_{\text{diode\_1}} + I_{\text{diode\_2}} + I_{\text{rec}} + I_{\text{sh}} - I_{\text{L}}, \tag{1}$$

where $I_{\text{diode\_1}}$ corresponds to the dark current of a high quality reference cell without cracks, $I_{\text{diode\_2}}$ corresponds to the dark current arising from cracks in the solar cell, I_{rec} is the current loss due to recombination through mid-gap defects, I_{sh} are the losses due to shunts and I_{L} is the photogenerated current density. The second diode is defined by (i) a value of the ideality factor n_2 and (ii) a dark current prefactor I_{02}. Here, the value of n_2 is equal to 2, such as for a recombination-limited p-i-n-type device, whereas I_{02} is the model parameter, which is used to fit the electrical IV characteristics and which will depend on the density of cracks in the intrinsic layer. The dark and illuminated IV curves were fitted using an in-house program (see details of the procedure in [61]). Estimation of the number of cracks was done over an average TEM cross-sectional length of 50 μm by analysis of adjacent micrographs. The p-i-n single-junction μc-Si:H cells were co-deposited by VHF PECVD at 200°C on the various substrates; the i-layer thickness was ~1.8 μm. Two significant results have been obtained: first, a clear correlation between crack density and I_{02} was established and, second, the decrease in open-circuit voltage (V_{oc}) and fill factor (FF) in the solar cells could be directly linked to an increase in crack density, as can be seen in Figures 5a and b, respectively.

Optimization of the TCO to be used with μc-Si:H material is hence under intensive investigation and comments will be given later in this paper about light-trapping (Section 4.1).

3.3. *Defects and material stability*

3.3.1. *Light-soaking*

During the initial stage of operation, the efficiency of amorphous silicon solar cells decreases due to the Staebler–Wronski effect, first observed in a-Si:H layers in 1977

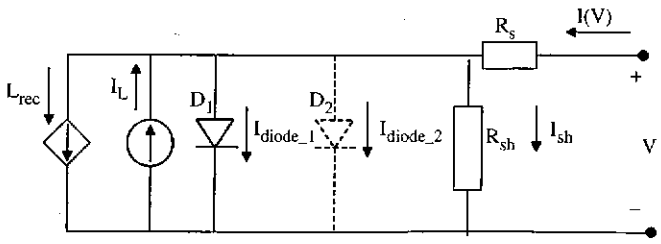

Figure 4. Equivalent electrical circuit for a μc-Si:H solar cell with an additional diode representing cracks.

[63]. After this initial phase of degradation, the efficiency stabilizes at 75–80% of the initial value for a single-junction cell. The light-induced defects created are metastable and light-induced degradation is observed to be completely reversible under thermal annealing; at temperatures above 150°C, only a few hours are sufficient to revert to the initial parameters. Created defects have been identified as additional dangling bonds that act as recombination centers; the increase in their density is responsible for the decrease observed in the efficiency of a-Si:H solar cells. It is commonly accepted now that the creation of dangling bonds is induced by the energy released when excess carriers recombine. Over the last decades, many models have been developed to explain the creation and annealing of such light-induced defects in a-Si:H, including the bond-breaking model [64–67], the dispersive model [68–70] or the hydrogen collision model [71]. Even though the models differ in some

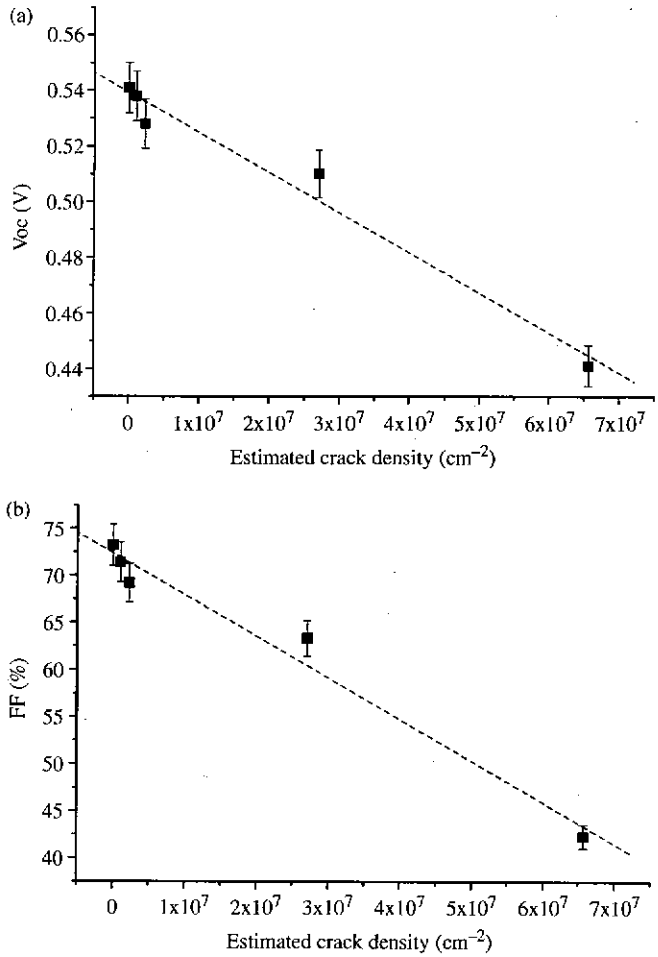

Figure 5. Decrease in the electrical parameters (V_{oc}, FF) of p-i-n single-junction μc-Si:H solar cells as a function of the crack density estimated from TEM micrographs [61]. Dotted lines are linear fits.

aspects, it is generally assumed that the diffusion of hydrogen plays a major role in the creation and annealing of dangling bonds.

On the other hand, μc-Si:H material, as used in the development of the first solar cell, was shown to be fully stable under light-soaking [9,72]. However, the i-layers had a high crystalline fraction. Complementary studies have demonstrated that with i-layers of medium crystallinity (40–60%), single-junction solar cells suffer from a mild form of light-induced degradation when exposed to blue or white light [73–77]. The light-induced degradation is larger for blue light (for constant short-circuit current density) due to a larger absorption in the amorphous phase and at the p–i interface, as discussed by Yan et al. [77], who additionally observed that μc-Si:H solar cells are fully stable when exposed to red light only. They concluded that only the amorphous phase of the material is responsible for the degradation [77]. The degradation observed under AM1.5 is dependent on the crystallinity of the μc-Si:H intrinsic layer, with a relative loss of efficiencies of up to 15% for solar cells containing intrinsic layers with a low crystalline volume fraction (<30%) [76]. However, further studies have suggested that small grains and/or intermediate-range order could also play an important role in the stability of μc-Si:H solar cells [78,79]. Furthermore, the degradation of the efficiency of solar cells is associated with an increase in defect-related absorption at 0.8 eV, as measured by the FTPS method (Figure 2). It should be noted that, even if μc-Si:H cells with a high crystalline volume fraction of the i-layer (>60%) are more stable, their initial and light-soaked values of $\alpha(0.8\,\text{eV})$ will be larger than those of cells with medium crystallinity.

The kinetics of light-induced degradation in μc-Si:H was recently studied to gain further insight into the exact microscopic mechanism behind this degradation effect

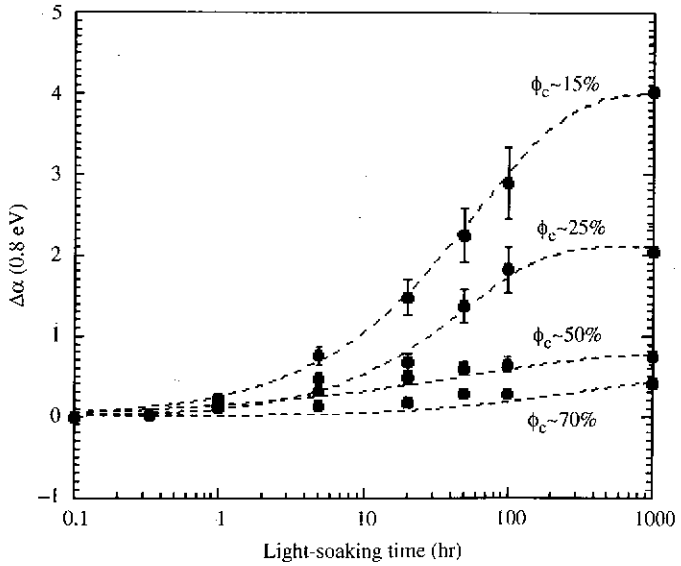

Figure 6. Relative increase in defect-related absorption as a function of light-soaking time for n-i-p single-junction μc-Si:H solar cells with i-layer crystalline volume fraction ϕ_c ranging from 15 to 70%. The dotted lines are fits according to stretched exponential functions.

[80]. It was demonstrated that, similarly to a-Si:H, both the kinetics of defect creation and annealing could be fitted with stretched exponential functions, as used in the dispersive model mentioned earlier. Note that similar kinetics were recently observed for defects present in a-Si:H/c-Si interfaces [81]. Such a stretched exponential function has the form (as given here for annealing):

$$N(t) = N(0) \cdot \exp\left[-\left(\frac{t}{\tau}\right)^{\beta}\right], \tag{2}$$

where N is the light-induced defect density, β and τ are the dispersive parameter and effective time constant, respectively.

Figure 6 presents the kinetics for the relative variation in defect-related absorption $\Delta\alpha$ (0.8 eV) (measured by FTPS and defined as $\Delta\dot{\alpha}(0.8\text{eV})(t) = (\alpha(t) - \alpha_{\text{initial}})/\alpha_{\text{initial}})$ in a series of n-i-p μc-Si:H solar cells. We observe, once again, that the defect-related absorption in the highly amorphous sample increases by a factor 4 after 1000 h of light-soaking (AM1.5-like spectrum at 50°C), whereas, in the case of high crystalline fraction, $\alpha(0.8\,\text{eV})$ remains almost constant.

The degradation and thermal recovery kinetics are slower than most a-Si:H layers, with larger values of the fit parameters (β, τ), which both depend on the crystalline volume fraction of the intrinsic layer material. We suggest that the stretched exponential kinetics could result from bond-breaking at the nanocrystals surface; the mechanism being mediated by dispersive diffusion of hydrogen within the amorphous phase. However, exact identification of the microscopic nature of light-induced defects in μc-Si:H is still lacking and further investigations with complementary experimental techniques, such as ESR [52,82], electrically detected

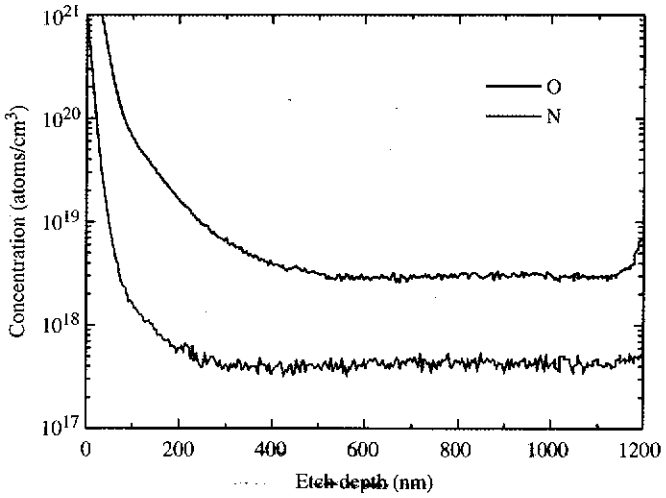

Figure 7. SIMS profiles of oxygen and nitrogen measured in a single junction μc-Si:H solar cell deposited under standard conditions in a large area PECVD reactor (silane concentration ~5%, power density ~0.15 W/cm^2 and deposition rate ~5 Å/s).

magnetic resonance (EDMR) [83] or photoluminescence (PL) spectroscopy [84], are necessary.

3.3.2. *Chemical contamination*

To obtain a sufficiently high value of the external quantum efficiency for μc-Si:H in the red and near-infrared range (800–1100 nm), the level of certain contaminants, such as oxygen or nitrogen, within the intrinsic layer must be kept low. Oxygen may be incorporated into layers through contamination of the feedstock gases and from the reactor walls; it becomes positively ionized and acts as an unintentional dopant. This typically affects the long wavelength part of the external quantum efficiency, where a dramatic loss is observed [85,86]. Note that nitrogen contamination acts very similarly on the performance of μc-Si:H solar cells; the critical contamination level being slightly lower [86]. Figure 7 shows a secondary ion mass spectroscopy (SIMS) profile for a state-of-the art μc-Si:H single-junction cell deposited in a large area PECVD reactor, indicating that the concentrations of oxygen and nitrogen are below the critical limits given in [86].

Other possible sources for contamination are: (i) air leaks and/or outgassing in the deposition chamber and (ii) *in situ* plasma cleaning procedures with, for example, SF_6/O_2 or NF_3. Finally, contamination may also occur from the doped layers, especially boron, which is used for the p-layer. In the p-i-n configuration, boron may, thus, contaminate the initial part of the intrinsic layer, especially if high deposition temperatures are used [87] or if the deposition of the i-layer is carried out directly in a single chamber system without particular care [88,89]. Boron contamination affects the carrier collection efficiency at the p–i interface and leads to a reduction in quantum efficiency in the short wavelength range, as well as a loss in open-circuit voltage and fill factor [90,91].

4. Microcrystalline silicon solar cells

In contrast to amorphous silicon, the production of commercial single-junction microcrystalline silicon modules has not received similar attention. However, μc-Si:H is widely used in tandem junctions with a-Si:H (see Section 5). We already mentioned two limiting factors of μc-Si:H, i.e. (i) the bandgap of ~1.1 eV that leads to lower open-circuit voltage values and (ii) an absorption coefficient that is larger in the near infrared but lower in the visible range, requiring a thicker intrinsic layer to obtain sufficient absorption (1–2 μm in μc-Si:H versus 0.2–0.3 μm for a-Si:H). Longer deposition times are, thus, necessary and lead to supplementary production costs. This will change if further progress is made towards more efficient light-trapping together with high material quality, and if deposition rates are further increased. Indeed, from a basic low deposition rate of ~1–2 Å/s, improvements have already allowed laboratories and equipment manufacturers to develop a first-generation process with typical deposition rates in the range 5–6 Å/s (for parallel plate PECVD), although it is desirable, for long term competitiveness, to reach 10 Å/s. Both light-trapping and deposition rate management will be discussed in the following sections, with the focus on μc-Si:H p-i-n cells.

4.1. *Light-trapping*

4.1.1. *Transparent conductive oxides properties*

The light management schemes used to reduce μc-Si:H i-layer thickness depend on the type of substrate considered and on the solar cell configuration: p-i-n or n-i-p. In the p-i-n configuration, glass coated with transparent conductive oxide (TCO) is the most common substrate, whereas in n-i-p configuration, flexible substrates, such as plastic foils, can be used, again in combination with various TCOs. For both solar cell configurations, the front TCO has to fulfill two major requirements: (i) high transparency in the useful spectral range to minimize optical losses by absorption (and/or by reflection) and (ii) high conductivity to limit the series resistance of the solar cell. Furthermore, especially in the case of p-i-n solar cells, the front TCO should be sufficiently rough (typical rms values between 50 and 200 nm) to (i) reduce reflections at the TCO/p-layer interface, thanks to refractive index grading, and (ii) increase the optical path of incoming light due to increased optical diffusion. This latter effect is critical for weakly absorbed light (800–1100 nm) that, furthermore, needs to be reflected at the back contact of the device. Multiple scattering at the TCO/silicon interfaces can result in, at least, a five-fold increase in the optical path within the intrinsic layer [92]. Thus, a larger value of TCO surface roughness generally leads to higher absorption and short-circuit current density values. However, as previously discussed in Section 3.2, TCO layers that are too rough with steep slopes typically lead to reduced values of V_{oc} and FF in a-Si:H [93] and μc-Si:H solar cells [14,94].

In practice, for high efficiency single-junction μc-Si:H cells, two materials are commonly used as front TCOs: indium tin oxide (ITO) for n-i-p μc-Si:H solar cells and ZnO for p-i-n cells. On the other hand, for p-i-n amorphous and micromorph solar cells and modules, a third TCO is widely used: fluorine-doped tin oxide (SnO_2:F). Here, we will focus on ZnO, which is typically deposited either by sputtering [95] or by low pressure chemical vapor deposition (LPCVD) [58,96] with aluminum and diborane as the usual dopants. The surface morphology differs depending on the deposition process; sputtered ZnO is

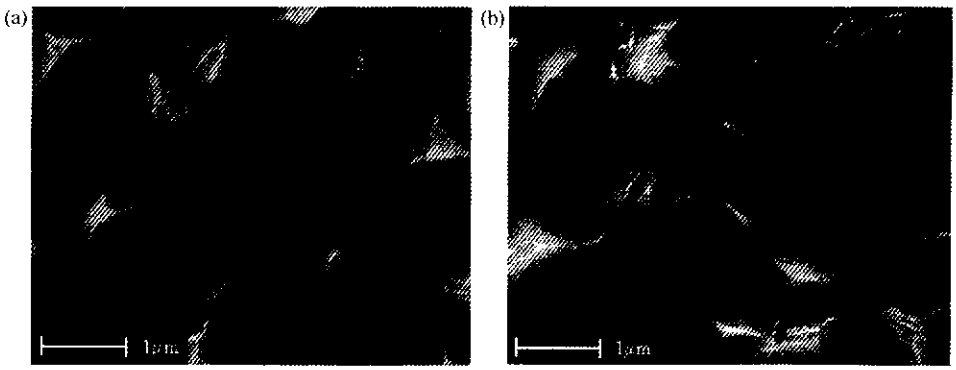

Figure 8. SEM micrographs of LPCVD zinc oxide surface (a) as-grown and (b) with plasma treatment for 40 min [14].

basically flat and needs a subsequent treatment (generally by wet etching) to increase its roughness. Via LPCVD, ZnO is rough as-grown, with a wurtzite crystalline structure and a pyramidal growth along the (110) axis, as can be seen from the scanning electron micrograph of the surface of a ~3 μm thick LPCVD ZnO layer in Figure 8a. The as-grown pyramidal surface morphology can be modified by applying a subsequent appropriate surface treatment, as shown in Figure 8b. Note that the LPCVD technique is relatively simple, and upscaling of deposition to areas larger than 1 m^2 has already been achieved, with deposition rates greater than 2 nm/s [97].

The optical transmission of ZnO layers is limited (a) in the short wavelength region and (b) in the near-infrared region because of the optical bandgap of ZnO (3.3 eV) and because of free carrier absorption. Hence, for use of zinc oxide as front contact, a compromise has to be found between the sheet resistance and the optical transmission. The sheet resistance can be reduced by increasing the layer thickness or the doping ratio but, in both cases, the optical absorption then increases. Similar tradeoffs are encountered with other TCO materials and the best way to solve this problem would be to achieve a higher carrier mobility. A possible solution lies in combining different TCO materials, as tested by J. Anna Selvan et al. [98], or in growing films with lowly doped large grains and high mobility, as reported by J. Steinhauser et al. [99].

4.1.2. *Anti-reflection layer at the TCO/Si interface*

In p-i-n μc-Si:H solar cells, the incident light is partially reflected at the air/glass, glass/ZnO and ZnO/silicon interfaces before being absorbed in the intrinsic silicon layer. Using Fresnel equations and assuming flat interfaces with negligible interference effects, a primary reflection of 4% at the air/glass interface, 2% at the

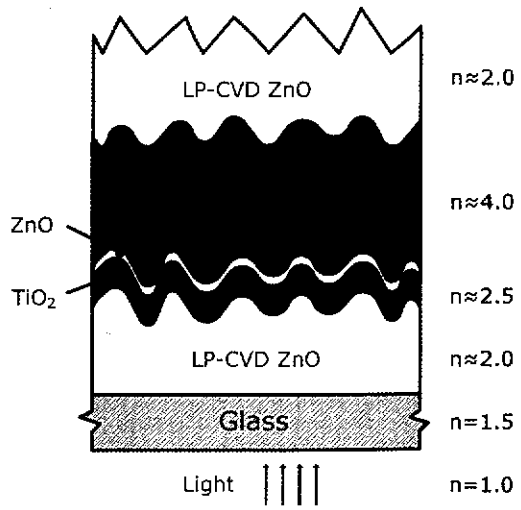

Figure 9. Schematic structure of a single-junction p-i-n μc-Si:H solar cell with LPCVD ZnO as front and back contact, and implantation of a TiO_2/ZnO bi-layer as an anti-reflection layer. Refractive index value for each layer is given as an indication.

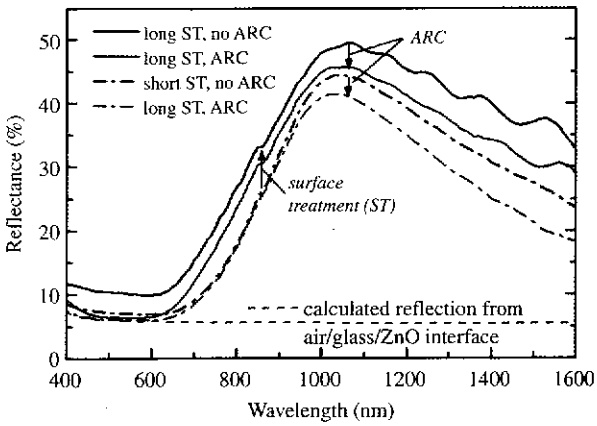

Figure 10. Reflectance of four single-junction p-i-n μc-Si:H cells from the same deposition run, with and without TiO_2/ZnO anti-reflection coating after front LPCVD ZnO. LPCVD ZnO was treated for short and long time periods with a surface treatment modifying the rms roughness and morphology: the longer the treatment, the lower the roughness [102].

glass/ZnO interface and 11% at the ZnO/silicon interface can be estimated. The first two reflections can be minimized with standard industrial anti-reflection coatings (ARC) on glass [100]. As an additional feature, one can use a TiO_2/ZnO stack as an ARC layer between the TCO and silicon layers, as first proposed by Matsui et al. [101] and recently investigated at IMT Neuchâtel [102]. In this last case, the TiO_2 and ZnO layers were both deposited by reactive RF sputtering; the ZnO layer is thin, in the order of 10 nm. The implantation of such an anti-reflection layer in a p-i-n type μc-Si:H solar cell is schematically presented in Figure 9. Using such a bi-layer ARC, the short-circuit current density of the μc-Si:H cell could be increased relatively by up to 4%. This corresponds to a total reflectance reduction from 10.2 to 6.4% at 550 nm, equivalent to reflectance at the glass interfaces only, as shown in Figure 10. However, we demonstrate in [102] that for a very rough TCO, which induces an efficient index grading, the effect of the bi-layer anti-refection coating is strongly reduced to near 1%. This can be seen in Figure 10, where the reflectance of p-i-n single junction μc-Si:H cells is shown for very rough (i.e. with a short surface treatment (ST) time, as presented in [14]) and less rough (long ST) front LPCVD ZnO.

4.2. *High deposition rates: developments and fabrication issues*

Deposition time currently constitutes a major cost factor in the production of amorphous silicon modules. Because microcrystalline silicon solar cells are substantially thicker than a-Si:H solar cells, deposition times are even more critical. As already indicated, deposition times can be lowered by (i) reducing the cell thickness through suitable light-trapping schemes and (ii) increasing deposition rates of μc-Si:H to over 10 Å/s. Following previous studies [103–107], a novel microcrystalline process regime for deposition at 10 Å/s, where RF power density

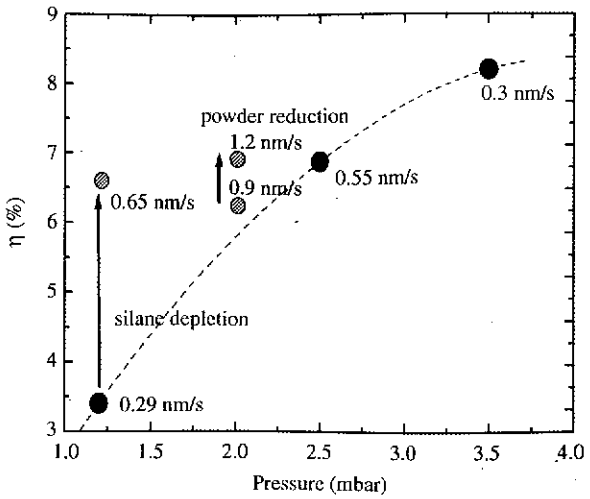

Figure 11. Single-junction μc-Si:H solar cell efficiencies as a function of deposition pressure (black dots). Grey dots are efficiencies obtained under high depletion conditions (where the ion energy is lower). The line is a guide for the eye.

is maintained at low values compared to other process regimes [29], was investigated at IMT Neuchâtel. It was observed that by increasing the pressure and silane depletion, microcrystalline material quality could be improved [106,108]. Higher pressure and silane depletion positively affect material quality under conditions where silane powder production remains negligible, whereas ion bombardment leads to amorphization of the μc-Si:H layer at low pressure and low silane depletion. A significant correlation between intrinsic material quality and solar cell efficiency was observed, and explained in terms of ion bombardment energy [106]. In fact, for reduced deposition pressures, the capacitive sheaths become less collisional, allowing ions with higher energies to impinge on the growing surface, leading to poorer material quality. On the other hand, in the case of higher silane depletion and higher pressure, plasma potential decreases and ion energy is also reduced. The correlation between ion bombardment and μc-Si:H material quality has been observed previously [34,107–109]. Figure 11 reviews the results obtained by IMT Neuchâtel during the development of various μc-Si:H solar cells [106]: the black dots on the line are solar cell efficiencies obtained under low depletion conditions at different pressures; the grey dots off the line are efficiencies obtained under high depletion conditions (where the ion energy is lower). The studies were performed in PECVD deposition reactors of a substrate size larger than $35 \times 45\,cm^2$, at 40.68 MHz, under conditions that allow for subsequent upscaling to areas larger than $1\,m^2$.

A clear trend can be observed in Figure 11 between deposition pressure and the conversion efficiency of μc-Si:H solar cells. Additionally, it is shown that increasing silane depletion at a given pressure (here 1.2 mbar) dramatically improves solar cell efficiency under conditions where powder formation is unimportant. At 2.0 mbar, powder formation became an issue in PECVD reactors and modifications were necessary to reduce it. To date, the best μc-Si:H cell efficiency obtained is 7.0% for a deposition rate of 12 Å/s and an i-layer thickness of 1.2 μm. Further improvements

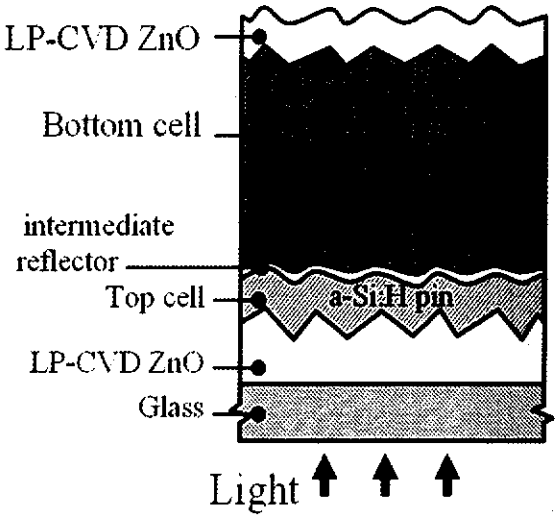

Figure 12. Schematic structure of a tandem a-Si:H/μc-Si:H p-i-n solar cell with LPCVD ZnO as front and back contacts, and with an intermediate reflector to enhance the top cell current.

in the plasma regime and μc-Si:H material quality are necessary to increase conversion efficiency, while maintaining a high deposition rate in a reactor of relatively large area. As will be seen in the next section, the utilization of such μc-Si:H cells in a tandem a-Si:H/μc-Si:H have already led to a promising initial efficiency value of 10.5% on 1.2 cm^2 [110]. These developments need to be implemented in larger area systems (> 1 m^2) and μc-Si:H layer uniformity checked. Indeed, it has already been demonstrated that good thickness and crystallinity homogeneity can be obtained on areas ranging from 1.4 m^2 [17] to 4.4 m^2 [111], but the situation is unclear for regimes with high deposition rates.

5. Microcrystalline/amorphous ('micromorph') tandem solar cell

Tandem and triple-junction solar cells are extensively used in amorphous silicon technology to obtain higher stabilized efficiencies than those attainable with single-junction solar cells. Tandem solar cells are especially attractive if the bandgap of each component cell can be properly adjusted. For amorphous silicon/amorphous silicon–germanium tandems, the major limitation concerns a further reduction in the bandgap, while maintaining good material quality and low value of light-induced degradation. On the other hand, microcrystalline silicon possesses a low bandgap value of ~1.1 eV, which, together with the 1.7–1.8 eV of a-Si:H, forms, in principle, an optimum combination for tandem cells [92].

In micromorph tandems, the thickness of the top a-Si:H cell has to be kept sufficiently thin to minimize the impact of light-induced degradation and its current, therefore, generally limits the current of the whole tandem device. The top amorphous cell displays major degradation, whereas the bottom μc-Si:H cell can be considered fully stable [112] since it is exposed to a lower illumination and, hence,

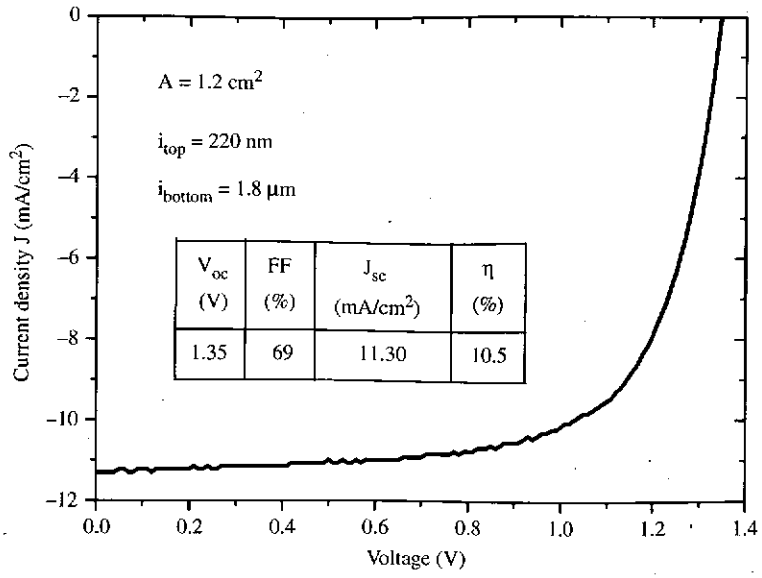

Figure 13. Initial *J–V* characteristics of a-SiH/µc-Si:H tandem solar cell deposited under high silane depletion conditions with *in situ* SiO-based intermediate reflector. The bottom µc-Si:H cell was deposited at 10 Å/s.

lower recombination rate. To overcome this issue of low current in the top cell, an intermediate reflective layer (IRL) can be introduced between the top and bottom cells, as schematically presented in Figure 12. The use of such an IRL in the a-Si:H/µc-Si:H tandem was previously proposed by IMT Neuchâtel in 1996 [113]. For a layer to act as an intermediate reflector, its refractive index must be lower than that of silicon to ensure light reflection at the interface. Moreover, the intermediate reflector must be sufficiently conductive to avoid electrical losses, but also as transparent as possible to minimize the absorption of light outside the active PV layers.

Zinc oxide was first used [114,115] as material for intermediate reflectors, but it has two major drawbacks for further industrialization: (i) it is deposited *ex situ* (not in the same reactor as the silicon layers) and (ii) an additional laser scribe is necessary for monolithic series interconnection to avoid lateral shunting of the segments. The development of an *in situ* intermediate reflector was presented by Yamamoto et al. [116] and fabrication of SiO-based intermediate reflectors has recently been reported under laboratory conditions [117,118]. Using such a SiO-based IRL and an anti-reflection coating on glass, a very high short-circuit current density value (J_{sc}) of 13.8 mA/cm^2 was obtained by IMT Neuchâtel in the top a-Si:H cell of a micromorph tandem cell with an i-layer thickness of 340 nm. Such a high J_{sc} value yielded a 13.3% initial conversion efficiency for the 1.2 cm^2 micromorph test cell [21].

In trials towards micromorph industrialization, a similar SiO-based IRL was developed directly in a large area KAI-S reactor, leading to a complete single-chamber process for the tandem. To date, a best initial conversion efficiency of 10.5% has been achieved with a µc-Si:H bottom cell of 1.8 µm deposited at 10 Å/s; the electrical characteristics are given in Figure 13. The short-circuit densities are

matched with 11.4 mA/cm^2 in the top cell and 11.3 mA/cm^2 in the bottom cell. Further improvements will have to be made regarding other cell parameters (V_{oc}, FF) and, more particularly, V_{oc}, which should be increased to values near 1.40 V.

The optimization of micromorph tandem cells is not an easy task since the stability of the tandem (and also the temperature coefficient) depends on which of the two partial cells is limiting the short-circuit current density (J_{sc}): the latter can be (i) limited by the top a-Si:H cell, (ii) limited by the bottom μc-Si:H cell or (iii) initially matched (both top and bottom cell current densities are equal). The first case is often avoided because it is expected to lead to larger light-induced degradation, although it was shown that this configuration could be more efficient in outdoor conditions due to differences in the spectral irradiance ratio and module temperature [119,120]. In the bottom limited case, the tandem tends to be matched after degradation, whereas the initially matched case will become top limited after degradation with a lower short-circuit current density, but possibly a higher FF value. Furthermore, indoor and outdoor testing may differ in the electrical conditions of light exposure performed under open-circuit conditions or at the maximum power point. Note that cells and, more particularly, modules should be designed ideally for optimal performance under given (usual) outdoor conditions (i.e. maximum number of annual kWh) and not for optimal stability under 'artificial' test conditions.

Finally, we advise that, although progress is needed in the fabrication of silicon layers (new plasma regimes with high deposition rate and high quality) to further increase conversion efficiency of microcrystalline silicon and micromorph cells and modules, the development of new, optimum TCOs is also necessary. The ideal TCO should allow for efficient light-trapping while leading to crack minimization and, hence, very high solar cell performances (V_{oc}, FF), such as typically obtained on flat substrates. By combining all these factors with anti-reflection layers and intermediate reflectors, stable efficiencies in the order of 13–14% should be achieved for micromorph tandem cells (with, for example, $V_{oc} = 1.42$ V, FF = 71%, $J_{sc} = 13.5$ mA/cm^2) instead of 11–12% as present.

6. Conclusions and prospects

Thin film silicon solar cells, both in amorphous and microcrystalline form, present the major advantages of (i) being based on abundant and non-toxic materials, (ii) allowing for low-temperature fabrication processes and (iii) having energy payback times much lower than those obtained for crystalline wafer-based silicon solar cells. Thin film silicon is, thus, a very promising material, with the potential of reaching lower module costs in terms of $/W$_p$ or €/W$_p$. Further cost reductions will be based on the assumption that larger deposition rates can be achieved, especially for microcrystalline silicon; thus, reaching higher machine throughputs. Indeed, the deposition time of μc-Si:H is now a key factor for its industrialization. As opposed to a-Si:H, μc-Si:H basically has the advantage of not being very sensitive to light-induced degradation, which leads to higher stabilized conversion efficiencies. At present, the optimum use of μc-Si:H is in combination with a-Si:H in micromorph tandems, where stable efficiencies above 11% have been obtained in the laboratory.

At the moment, the main research priorities for thin film silicon solar cells are focused on reducing the cost of μc-Si:H by increasing the deposition rate and decreasing the thickness of the intrinsic layer. The latter parameter requires the development of better light-trapping schemes through (i) improved and/or new TCOs that allow for efficient light-trapping and good 'crackless' growth properties, (ii) further progress in the properties and fabrication of anti-reflection layers and intermediate reflectors. New materials also need to be developed for triple junction cells and modules: basically, a stable material with an appropriate intermediate bandgap value in the range of 1.5 eV, while avoiding the use of germanium.

Acknowledgements

The authors gratefully acknowledge financial support from the European Union through the project 'ATHLET', the Swiss Federal Office of Energy and the Swiss National Science Foundation.

References

[1] V. Fthenakis, S. Gualtero, R. van der Meulen and H.C. Kim, Proc. Mater. Res. Soc. Symp. 1041 (2007) p.R01.
[2] R.C. Chittick, J.H. Alexande and H.F. Sterling, J. Electrochem. Soc. 116 (1969) p.77.
[3] D.E Carlson, C.R. Wronski and J.I. Pankove, RCA Rev. 38 (1977) p.211.
[4] S. Veprek and V. Marecek, Solid State Electron. 11 (1968) p.683.
[5] W.E. Spear, G. Willeke and P.G LeComber, J. Phys. Colloques 42 (NC4) (1981) p.257.
[6] C. Droz, E. Vallat-Sauvain, J. Bailat, L. Feitknecht, J. Meier, X. Niquille and A. Shah, *Proceedings of the 3rd WCPE*, Osaka, Japan, 2003, p.1544.
[7] G. Lucovsky, C. Wang, R.J. Nemanich and M.J. Williams, Sol. Cells 30 (1991) p.419.
[8] M. Faraji, S. Gokhale, S.M. Choudhari, M.G. Takwale and S.V. Ghaisas, Appl. Phys. Lett. 60 (1992) p.3289.
[9] J. Meier, P. Torres, R. Platz, S. Dubail, U. Kroll, J.A.A. Selvan, N. Pellaton-Vaucher, C. Hof, D. Fischer, H. Keppner, A. Shah, K.-D. Ufert, P. Giannoules and J. Kohler, Proc. Mater. Res. Soc. Symp. 420 (1996) p.3.
[10] P. Torres, J. Meier, M. Goetz, N. Beck, U. Kroll, H. Keppner and A. Shah, Proc. Mater. Res. Soc. Symp. 452 (1997) p.883.
[11] R. Martins and G. Willeke, Proc. Mater. Res. Soc. Symp. 149 (1989) p.369.
[12] M. Wen, C.L. Chin, T. Saida, H. Okamoto and Y. Hamakawa, *Technical Digest of the 7th PVSEC*, Nagoya, Japan, 1993, p.267.
[13] Y. Mai, S. Klein, J. Wolff, A. Lambertz, X. Geng and F. Finger, *Proceedings of the 19th EUPVSEC*, Paris, France, 2004, p.1399.
[14] J. Bailat, D. Dominé, R. Schlüchter, J. Steinhauser, S. Faÿ, F. Freitas, C. Bücher, L. Feitknecht, X. Niquille, T. Tscharner, A. Shah and C. Ballif, *Proceedings of the 4th WCPEC*, Hawaii, USA, 2006, p.1533.
[15] K. Yamamoto, M. Toshimi, T. Suzuki, Y. Tawada, T. Okamoto and A. Nakajima, Proc. Mater. Res. Soc. Symp. 507 (1998) p.131.
[16] J. Meier, J. Spitznagel, U. Kroll, C. Bucher, S. Faÿ, T. Moriarty and A. Shah, Thin Solid Films 451/452 (2004) p.518.
[17] U. Kroll, J. Meier, S. Benagli, D. Borrello, J. Hötzel, J. Spitznagel, B. Dehbozorgi, H. Schmidt, G. Monteduro, O. Kluth, R. Kravets, M. Kupich, C. Ellert, S. Bakehe,

H. Goldbach, M. Keller, T. Roschek, L. Schmid, W. Burkhardt, B. Gilles, J. Springer, D. Zimin, G. Buechel, A. Hügli, A. Zindel, T. Kratzla and D. Koch-Ospelt, *Proceedings of the 22nd EUPVSEC*, Milano, Italy, 2007, p.1795.

[18] J. Meier, S. Dubail, R. Flückiger, D. Fischer, H. Keppner and A. Shah, *Proceedings of the 1st WCPEC*, Hawaii, USA, 1994, p.409.

[19] J. Meier, P. Torres, R. Platz, S. Dubail, U. Kroll, J.A.A. Selvan, N. Pellaton-Vaucher, C. Hof, D. Fischer, H. Keppner, A. Shah and K.D. Ufert, Sol. Energ. Mater. Sol. Cells 49 (1997) p.35.

[20] B. Rech, T. Roschek, T. Repmann, J. Müller, R. Schmitz and W. Appenzeller, Thin Solid Films 427 (2003) p.157.

[21] D. Dominé, P. Buehlmann, J. Bailat, A. Billet, A. Feltrin and C. Ballif, *Proceedings of the 23rd EUPVSEC*, Valencia, Spain, 2008.

[22] J. Meier, U. Kroll, S. Benagli, J. Hötzel, J. Bailat, D. Borrello, J. Spitznagel, L. Castens, E. Vallat-Sauvain, B. Dehbozorgi, O. Kluth, R. Kravets, M. Kupich, C. Ellert, S. Bakehe, H. Goldbach, M. Keller, T. Roschek, M. Gossla, H. Knauss, T. Eisenhammer and J. Henz, *Proceedings of the 23rd EUPVSEC*, Valencia, Spain, 2008.

[23] K. Yamamoto, A. Nakajima, M. Yoshimi, T. Sawada, S. Fukuda, T. Suezaki, M. Ichikawa, Y. Koi, M. Goto, H. Tanaka, T. Sasaki and Y. Tawada, *Proceedings of the 3rd WCPEC*, Osaka, Japan, 2003, S2OB903.

[24] M. Yoshimi, T. Sasaki, T. Sawada, Z. Suezaki, T. Meguro, T. Matsuda, K. Santo, K. Wadano, M. Ichikawa, A. Nakajima and K. Yamamoto, *Proceedings of the 3rd WCPEC*, Osaka, Japan, 2003, p.1566.

[25] H. Curtins, N. Wyrsch, M. Favre and A.V. Shah, Plasma Chem. Plasma Process. 7 (1987) p.267.

[26] R. Zedlitz, M. Heintze and G.H. Bauer, Proc. Mater. Res. Soc. 258 (1992) p.147.

[27] A.A. Howling, J.-L. Dorier, Ch. Hollenstein and U. Kroll, J. Vac. Sci. Tech. A 10 (1992) p.1080.

[28] W.G.J.H.M. van Sark, J. Bezemer and W.F. van der Weg, Surf. Coatings Tech. 74/75 (1995) p.63.

[29] A. Smets, T. Matsui and M. Kondo, J. Appl. Phys. 104 (2008) p.034508.

[30] M. Heintze and R. Zedlitz, J. Non-Cryst. Solid. 164/166 (1993) p.55.

[31] M. Kondo, M. Fukawa, K. Saitoh and A. Matsuda, Jpn. J. Appl. Phys. 37 (1998) p.L1116.

[32] B. Rech, T. Roschek, J. Müller, S. Wieder and H. Wagner, Sol. Energ. Mater. Sol. Cells 66 (2001) p.267.

[33] U. Graf, J. Meier, U. Kroll, J. Bailat, C. Droz, E. Vallat-Sauvaina and A. Shah, Thin Solid Films 427 (2003) p.37.

[34] T. Matsui, A. Matsuda and M. Kondo, Sol. Energ. Mater. Sol. Cells 90 (2006) p.3199.

[35] Y. Nakano, S. Goya, T. Wanabe, N. Yamashita and Y. Yonekura, Thin Solid Films 506/507 (2006) p.33.

[36] Y. Ide, Y. Saito, A. Yamada and M. Konagai, *Proceedings of the 3rd WCPEC*, Osaka, 2003, p.1772.

[37] S. Klein, T. Repmann and T. Brammer, Sol. Energ. 77 (2004) p.893.

[38] H. Hakuma, K. Niira, H. Senta, T. Nishimura, M. Komoda, H. Okui, K. Amaraki, Y. Okada, K. Tornita, H. Higutchi and H. Arimune, *Proceedings of the 3rd WCPEC*, Osaka, 2003, p.1796.

[39] Y. Mai, S. Klein, R. Carius, H. Stiebig, X. Geng and F. Finger, Appl. Phys. Lett. 87 (2005) p.073503.

[40] H. Shirai, G. Ohkawara and M. Nakajima, Solid State Phenom. 93 (2003) p.109.

[41] B. Yan, G. Yue, J. Yang, K. Lord, A. Banerjee and S. Guha, *Proceedings of the 3rd WCPEC*, Osaka, Japan, 2003, p.2773.

[42] L. Feitknecht, J. Meier, P. Torres, J. Zürcher and A. Shah, Sol. Energ. Mater. Sol. Cells 74 (2002) p.539.
[43] M.N. van den Donker, B. Rech, F. Finger, W.M.M. Kessels and C.M. van de Sanden, Appl. Phys. Lett. 87 (2005) p.263503.
[44] E. Vallat-Sauvain, U. Kroll, J. Meier, A. Shah and J. Pohl, J. Appl. Phys. 87 (2000) p.3137.
[45] U. Kroll, J. Meier, P. Torres, J. Pohl and A. Shah, J. Non-Cryst. Solid. 227/230 (1998) p.68.
[46] L. Houben, M. Luysberg, P. Hapke, R. Carius, F. Finger and H. Wagner, Phil. Mag. A 77 (1998) p.1447.
[47] P. Roca i Cabarrocas, N. Layadi, T. Heitz, B. Drévillon and I. Solomon, Appl. Phys. Lett. 66 (1995) p.3609.
[48] K. Mori, T. Yasuda, M. Nishizawa, S. Yamasaki and K. Tanaka, Jpn. J. Appl. Phys. 39 (2000) p.6647.
[49] J. Bailat, E. Vallat-Sauvain, L. Feitknecht, C. Droz and A. Shah, J. Non-Cryst. Solid. 299/302 (2002) p.1219.
[50] M. Vanecek and A. Poruba, Appl. Phys. Lett. 80 (2002) p.719.
[51] A. Poruba, M. Vanecek, J. Meier and A. Shah, J. Non-Cryst. Solid. 299/302 (2002) p.536.
[52] M. Vanecek, A. Poruba, Z. Remes, J. Rosa, S. Kamba, V. Vorlícek, J. Meier and A. Shah, J. Non-Cryst. Solid. 266/269 (2000) p.519.
[53] N. Wyrsch, F. Finger, T.J. McMahon and M. Vanecek, J. Non-Cryst. Solid. 137/138 (1991) p.347.
[54] A.L. Baia Neto, A. Lambertz, R. Carius and F. Finger, J. Non-Cryst. Solid. 299/302 (2002) p.274.
[55] F. Meillaud, E. Vallat-Sauvain, X. Niquille, D. Dominé, A. Shah and C. Ballif, *Proceedings of the 21st EUPVSEC*, Dresden, Germany, 2006, p.1729.
[56] H. Keppner, P. Torres, R. Flückiger, A. Shah, C. Fortmann, P. Fath, G. Willeke, K. Happle and H. Kiess, Sol. Energ. Mater. Sol. Cells 34 (1994) p.201.
[57] M. Python, E. Vallat-Sauvain, J. Bailat, C. Ballif and A. Shah, Proc. Mater. Res. Soc. Symp 910 (2006) p.0910-A13-02.
[58] S. Faÿ, U. Kroll, C. Bucher, E. Vallat-Sauvain and A. Shah, Sol. Energ. Mater. Sol. Cells 86 (2005) p.385.
[59] M. Luysberg, C. Scholten, L. Houben, R. Carius, F. Finger and O. Vetterl, Proc. Mater. Res. Soc. Symp. 664 (2001) p.A15.2.
[60] J. Löffler, A. Gordijn, R.L. Stolk, H. Li, J.K. Rath and R.E.I. Schropp, Sol. Energ. Mater. Sol. Cells 87 (2005) p.251.
[61] M. Python, E. Vallat-Sauvain, J. Bailat, D. Dominé, L. Fesquet, A. Shah and C. Ballif, J. Non-Cryst. Solid. 354 (2007) p.2258.
[62] J. Merten, J.M. Asensi, C. Voz, A.V. Shah, R. Platz and J. Andreu, IEEE Trans. Electron. Devices 45 (1998) p.423.
[63] D.L. Staebler and C.R.J. Wronski, Appl. Phys. Lett. 31/4 (1977) p.292.
[64] I. Hirabayashi, K. Morigaki and S. Nitta, Jpn. J. Appl. Phys. 19 (1980) p.L357.
[65] J.I. Pankove and J.E. Berkeyheiser, Appl. Phys. Lett. 37 (1980) p.705.
[66] M. Stutzmann, W.B. Jackson and C.C. Tsai, Phys. Rev. B 32 (1985) p.23.
[67] B. Ross, J. Deng, M.L. Albert, R.W. Collins and C.R. Wronski, *Proceedings of the 4th WCPEC*, Hawaii, 2006, p.1576.
[68] D. Redfield and R.H. Bube, Appl. Phys. Lett. 54 (1989) p.1037.
[69] W.B. Jackson and J. Kakalios, Phys. Rev. B 37 (1988) p.1020.
[70] K. Morigaki and F. Yonezawa, J. Non-Cryst. Solid. 164/166 (1993) p.215.
[71] H. Branz, Solid State Commun. 105 (1998) p.387.
[72] K. Yamamoto, IEEE Trans. Electron. Devices 46 (1999) p.2041.

[73] P. St'ahel, S. Hamma, P. Sladek and P. Roca i Cabarrocas, Sol. Energ. Mater. Sol. Cells 227/230 (1998) p.276.
[74] S. Klein, F. Finger, R. Carius and H. Stiebig, *Proceedings of the 19th EUPVSEC*, Paris, France, 2004, p.1579.
[75] F. Meillaud, E. Vallat-Sauvain, X. Niquille, M. Dubey, J. Bailat, A. Shah and C. Ballif, *Proceedings of the 31st IEEE PVSEC*, Orlando, FL, USA, 2005, p.1412.
[76] F. Meillaud, E. Vallat-Sauvain, X. Niquille, M. Dubey, A. Shah and C. Ballif, *Proceedings of the 20th EUPVSEC*, Barcelona, Spain, 2005, p.1509.
[77] B. Yan, G. Yue, J.M. Owens, J. Yang and S. Guha, Appl. Phys. Lett. 85 (2004) p.1925.
[78] G. Yue, B. Yan, G. Ganguly, J. Yang, S. Guha and C.W. Teplin, Appl. Phys. Lett. 88 (2006) p.263507.
[79] G. Yue, B. Yan, G. Ganguly, J. Yang and S. Guha, J. Mater. Res. 22 (2007) p.1128.
[80] F. Meillaud, E. Vallat-Sauvain, A. Shah and C. Ballif, J. Appl. Phys. 103 (2008) p.054504.
[81] S. de Wolf, S. Olibet and C. Ballif, Appl. Phys. Lett. 93 (2008) p.032101.
[82] K. Morigaki and C. Niikura, Solid State Commun. 136 (2005) p.308.
[83] C. Boehme and K. Lips, J. Non-Cryst. Solid. 338 (2004) p.434.
[84] T. Merdzhanova, R. Carius, S. Klein, F. Finger and D. Dimova-Malinovska, Thin Solid Films 511/512 (2006) p.394.
[85] P. Torres, J. Meier, R. Flückiger, U. Kroll, J.A.A. Selvan, H. Keppner, A. Shah, S.D. Littlewood, I.E. Kelly and P. Giannoules, Appl. Phys. Lett. 69 (1996) p.1373.
[86] T. Kilper, M.N. van den Donker, D. Grunsky, A. Mück, R. Schmitz, U. Zastrow, B. Rech, G. Bräuer, S. Klein and T. Repmann, *Proceedings of the 21st EUPVSEC*, Dresden, Germany, 2006, p.1738.
[87] M. Kondo, T. Matsui, Y. Nasuno, C. Niikura, T. Fujibayashi, A. Sato, A. Matsuda and H. Fujiwara, *Proceedings of the 31st IEEE PVSEC Conference*, Orlando, FL, USA, 2005, p.1377.
[88] P. Roca i Cabarrocas, S. Kumar and B. Drevillon, J. Appl. Phys. 66 (1989) p.3286.
[89] U. Kroll, C. Bucher, S. Benagli, I. Schönbächler, J. Meier, A. Shah, J. Ballutaud, A. Howling, Ch. Hollenstein, A. Büchel and M. Poppeller, Thin Solid Films 451/452 (2004) p.525.
[90] J. Ballutaud, C. Bucher, Ch. Hollenstein, A.A. Howling, U. Kroll, S. Benagli, A. Shah and A. Buechel, Thin Solid Films 468 (2004) p.222.
[91] L. Feitknecht, F. Freitas, C. Bucher, J. Bailat, A. Shah, C. Ballif, J. Meier, J. Spitznagel, U. Kroll, B. Strahm, A.A. Howling, L. Samsonnens and C. Hollenstein, *Proceedings of the 21st EUPVSEC*, Dresden, Germany, 2006, p.1634.
[92] A. Shah, M. Vanecek, J. Meier, F. Meillaud, J. Guillet, D. Fischer, C. Droz, X. Niquille, S. Faÿ, E. Vallat-Sauvain, V. Terrazzoni-Daudrix and S. Faÿ, J. Non-Cryst. Solid. 338/340 (2004) p.639.
[93] O. Kluth, B. Rech, L. Houben, S. Wieder, G. Schope, C. Beneking, H. Wagner, A. Loffl and H.W. Schock, Thin Solid. Films 351 (1999) p.247.
[94] Y. Nasuno, M. Kondo and A. Matsuda, Jpn. J. Appl. Phys. 40 (2001) p.L303.
[95] J. Müller, B. Rech, J. Springer and M. Vanecek, Sol. Energ. 77 (2004) p.917.
[96] R.G. Gordon, in NREL/SNL Photovoltaics Program Review of the 14th Conference A Joint Meeting, Lakewood, CO, USA, 1997, p.39.
[97] O. Kluth, H. Kuhn, D. Zimin, M. Poppeller, D. Plesa, T. Roschek, J. Springer, W. Stein, A. Buechel, U. Kroll, A. Huegli, D. Borrello, G. Androutsopoulos, S. Benagli and J. Meier, *Proceedings of the 20th EUPVSEC*, Barcelona, Spain, 2005, p.1659.
[98] J.A.A. Selvan, Y.-M. Li, S. Guo and A.E. Delahoy, *Proceedings of the 19th EU PVSEC*, Paris, France, 2004, p.1346.
[99] J. Steinhauser, L. Feitknecht, S. Faÿ, R. Schlüchter, J. Springer, A. Shah and C. Ballif, *Proceedings of the 20th EU PVSEC*, Barcelona, Spain, 2005, p.1608.

[100] H.J. Gläser, *Large Area Glass Coatings*, Von Ardenne Anlagentechnik GmbH, Dresden, 2000.
[101] T. Matsui, T. Fujibayashi, A. Sato, H. Sonobe and M. Kondo, *Proceedings of the 20th EUPVSEC*, Barcelona, Spain, 2005, p.1493.
[102] P. Buehlmann, A. Billet, J. Bailat and C. Ballif, *Proceedings of the 22nd EUPVSEC*, Milano, Italy, 2007, p.2182.
[103] B. Strahm, A.A. Howling, L. Sansonnens, Ch. Hollenstein, U. Kroll, J. Meier, Ch. Ellert, L. Feitknecht and C. Ballif, Sol. Energ. Mater. Sol. Cells 91 (2007) p.495.
[104] M.N. Van den Donker, B. Rech, F. Finger, L. Houben, W.M.M. Kessels and M.C.M. van de Sanden, Prog. Photovolt. 15 (2007) p.291.
[105] L. Feitknecht, F. Freitas, C. Bucher, J. Bailat, A. Shah, C. Ballif, J. Meier, J. Spitznagel, U. Kroll, B. Strahm, A.A. Howling, L. Samsonnens and C. Hollenstein, *Proceedings of the 21st EUPVSEC*, Dresden, Germany, 2006, p.1634.
[106] A. Feltrin, G. Bugnon, F. Meillaud, J. Bailat and C. Ballif, *Proceedings of the 23rd EUPVSEC*, Valencia, Spain, 2008.
[107] A. Gordijn, L. Hodakova, J.K. Rath and R.E.I. Schropp, J. Non-Cryst. Solid. 352 (2006) p.1868.
[108] M. Kondo, Sol. Energ. Mater. Sol. Cells 78 (2003) p.543.
[109] A.H.M. Smets and M. Kondo, J. Non-Cryst. Solid. 352 (2006) p.937.
[110] F. Meillaud, A. Feltrin, G. Bugnon, G. Parascandolo, P. Buehlmann and C. Ballif, *Proceedings of the 23rd EUPVSEC*, Valencia, Spain, 2008.
[111] Y. Chae, T.K. Won, L. Li, S. Sheng, S.Y. Choi, J. White and M. Frei, *Proceedings of the 22nd EUPVSEC*, Milano, Italy, 2007, p.1807.
[112] N. Pellaton-Vaucher, J.-L. Nagel, R. Platz, D. Fischer and A. Shah, *Proceedings of 2nd WCPEC*, Vienna, 1998, p.728.
[113] D. Fischer, S. Dubail, J.A.A. Selvan, N. Pellaton Vaucher, R. Platz, Ch. Hof, U. Kroll, J. Meier, P. Torres, H. Keppner, N. Wyrsch, M. Goetz, A. Shah and K.D. Ufert, *Proceedings of the 25th IEEE PVSEC*, Washington, DC, 1996, p.1053.
[114] D. Dominé, J. Bailat, J. Steinhauser, A. Shah and C. Ballif, *Proceedings of the 4th WPCEC*, Hawaii, 2006, p.1465.
[115] S.Y. Myong, K. Sriprapha, S. Miyajima and M. Konagai, Appl. Phys. Lett. 90 (2007) p.263509.
[116] K. Yamamoto, A. Nakajima, M. Yoshimi, T. Sawada, S. Fukuda, T. Suezaki, M. Ichikawa, Y. Koi, M. Goto, T. Meguro, T. Matsuda, M. Kondo, T. Sasaki and Y. Tawada, Prog. Photovolt. 13 (2005) p.645.
[117] A. Lambertz, A. Dasgupta, W. Reetz, A. Gordijn, R. Carius and F. Finger, *Proceedings of the 22nd EUPVSEC*, Milano, Italy, 2007, p.1839.
[118] P. Buehlmann, J. Bailat, D. Dominé, A. Billet, F. Meillaud, A. Feltrin and C. Ballif, Appl. Phys. Lett. 91 (2007) p.143505.
[119] A. Nakajima, M. Ichikawa, T. Sawada, M. Yoshimi and K. Yamamoto, Jpn. J. Appl. Phys. 43 (2004) p.L1162.
[120] K. Yamamoto, A. Nakajima, M. Yoshimi, T. Sawada, S. Fukuda, T. Suezaki, M. Ichikawa, Y. Koi, M. Goto, T. Miguro, T. Matsuda, M. Kondo, T. Sasaki and Y. Tawada, *Proceedings of the 31st IEEE PVSC*, Orlando, FL, USA, 2005, p.1468.